PNAS RESEARCH ARTICLE | APPLIED PHYSICAL SCIENCES

Cooperative transitions involving hydrophobic polyelectrolytes

James L. Martin Robinson[a] and Willem K. Kegel[a,1]

Edited by Daan Frenkel, University of Cambridge, Cambridge, UK; received June 28, 2022; accepted December 16, 2022

Hydrophobic polyelectrolytes (HPEs) can solubilize bilayer membranes, form micelles, or can reversibly aggregate as a function of pH. The transitions are often remarkably sharp. We show that these cooperative transitions occur by a competition between two or more conformational states and can be explained within the framework of Monod–Wymann–Changeux (MWC) theory that was originally formulated for allosteric interactions. Here, we focus on the pH-dependent destabilization and permeation of bilayer membranes by HPEs. We formulate the general conditions that lead to sharp conformational transitions involving simple macromolecules mediated by concentration variations of molecular ligands. That opens up potential applications ranging from medicine to the development of switchable materials.

hydrophobic polyelectrolytes | cooperativity | membrane solubilization

Significance

Sharp, cooperative, switch-like transitions are key in biological regulation. A textbook example is the sensitivity of the binding of oxygen onto hemoglobin. It is generally assumed that only complex molecules such as proteins display these type of cooperative transitions, which are driven by an underlying conformational change. We show that the interactions between protons and relatively simple hydrophobic polyelectrolytes can be described under the same theoretical framework, and we detail the conditions that lead to sharp, pH-induced transitions. These findings are potentially relevant in drug and gene delivery applications and in the development of materials whose optical, electronic, or other properties can be switched by small concentration variations of molecular ligands.

Hydrophobic polyelectrolytes (HPEs) are (bio) polymers that consist of hydrophobic as well as ionic (weak acids or bases) functional groups that are either part of the same side group or homogeneously distributed over the polymer chain (*SI Appendix*, Table S1) (1, 2). The main characteristic of the transitions involving HPEs is their cooperative nature, or sharpness, as a function of *pH*.

In biology, small molecular ligands often bind to larger substrates, typically protein molecules, in a cooperative manner. These allosteric interactions can lead to sharp transitions between the unbound (without ligands) and bound states of a substrate (3). The bound and unbound states are often related to some activity of the substrate; for example, low-molecular-weight ligands can be activators or inhibitors of an enzyme (4). In that way, sharp activity switches, or "on" and "off" states, are possible as a function of the concentration of one or more ligands (5). A textbook example of a cooperative binding transition is the allosteric binding of oxygen to hemoglobin in red blood cells. If there was no cooperativity (allostery) in the binding of oxygen molecules to the four binding sites of hemoglobin, the transition from unbound oxygen to complete saturation of all the four binding sites would occur over a relatively broad range in oxygen pressure. A model for the sharp transition over a relatively narrow range of oxygen pressure has been put forward by Monod et al. (6), referred to as MWC theory. In that description, hemoglobin can be in (at least) two conformation states: one with low affinity for oxygen (the tense or T state) and one with relatively high affinity (the relaxed or R state). The last conformation is unfavorable at low oxygen concentrations but becomes favorable when several oxygen molecules bind. *SI Appendix*, *Theory* for a detailed description of MWC applied to hemoglobin. While it is likely that the oxygen-binding sites of hemoglobin somehow interact, this is not a necessary assumption. In fact, in the original MWC paper (6), no assumptions have been made regarding the interactions between oxygen-binding sites. The only necessary requirement is that there are two conformational states, one of which is unfavorable at low oxygen pressure and becomes stable by binding more than one oxygen molecule. With that in mind, one may expect that cooperative transitions are not limited to complex substrates such as proteins but may also occur in relatively simple substrates as long as there are well-defined conformation states, each with different binding affinity for ligands. This is what we will demonstrate in this work. A singular observation of cooperative binding by, likely, an MWC mechanism, has been reported on the binding of low-molecular-weight ligands onto aggregates of modified cyclodextrins (7). An example of a mechanism other than MWC that can also cause sharp transitions in relatively simple substrates and ligands is by (weak) multivalent interactions, see, e.g., ref. 8 and 9. In these systems, the transitions are driven by combinatorial entropy of multiple binding sites of both ligands and substrates (or receptors in the terminology in ref. 8). Here, we will focus on hydrophobic polyelectrolytes as relatively simple substrates that can show cooperative transitions driven by the concentration of potential determining ions. One conformation state of a hydrophobic polyelectrolyte chain is a hydrophobic state, where the ionizable groups in the polymer have a low affinity for potential determining ions, being protons in the case of

Author affiliations: [a]Van't Hoff Laboratory for Physical and Colloid Chemistry, Debye Institute for Nanomaterials Science, Utrecht University, Utrecht 3584 CH, The Netherlands

Author contributions: W.K.K. designed research; J.L.M.R. and W.K.K. performed research; J.L.M.R. analyzed data; and J.L.M.R. and W.K.K. wrote the paper.

The authors declare no competing interest.

This article is a PNAS Direct Submission.

[1]To whom correspondence may be addressed. Email: w.k.kegel@uu.nl.

This article contains supporting information online at http://www.pnas.org/lookup/suppl/doi:10.1073/pnas.2211088120/-/DCSupplemental.

Published January 30, 2023.

basic side groups and hydroxyl ions for acidic groups. Another conformation can be an aqueous state which is unfavorable at low concentrations of potential determining ions but has a high affinity for these ions and becomes stable upon binding several ions at once. Other conformations may also occur, such as HPEs localized at the rim of a bilayer disk.

In the following, we formulate MWC theory in terms of the properties of HPEs and compare our model to the experimental behavior of hydrophobic polyelectrolytes in several guises: 1) micellization of HPEs in the form of diblock copolymers, 2) the globule–coil transition in aqueous solutions, and 3) disk formation and permeation in lipid bilayer membranes. If it is possible to control transition pH and the width of the pH region where the transitions occur (the sharpness or degree of cooperativity), it will open up new routes to the development of artificial drug and gene delivery vehicles and cancer treatment; see a review of pH-responsive tumor-targeted approaches (10) and *SI Appendix, Applications* for more details. In a broader perspective, the ability to switch between states with different optical, electronic, or other properties driven by (very) small concentration variations of relevant molecular ligands may aid in the development of materials.

Theory

In *SI Appendix, Theory*, we generalize MWC theory to situations in which substrates can have multiple states. In the case of HPEs, we define a hydrophobic state as the ground state in which ionization is prohibitively unfavorable. The aqueous state is unfavorable in terms of interactions between the hydrophobic side groups of the polymers with water. On the other hand, in that state, ionization, or binding of potential determining ions (protons or hydroxyl ions), is favorable. Transitions between these states are brought about by the changes in the concentrations of potential determining ions such as proton concentration, that is, pH. We can identify analogous transitions in the form of micellization of hydrophilic–hydrophobic polyelectrolyte diblocks or the permeation and solubilization of membranes. We have schematically sketched these transitions in Fig. 1.

The model we propose for the ionization transition is based on the Monod–Wyman–Changeux (MWC) theory for allosteric transitions (6), as described in *SI Appendix, Theory*. We take the ionization of (weak) acid groups on the polymers as the binding of ligands in the form of hydroxyl ions*. In the case of basic ionizable groups on the polymer, protons are the ligands. These (hydroxyl or proton) ligands play the role of oxygen in binding onto hemoglobin. We essentially neglect ionization in the hydrophobic state of the polymers, being similar to assuming a very low affinity for ligands in the form of ions. The statistical weight of an HPE in the aqueous state in the form of the coarse-grained grand partition function is given by, *SI Appendix*, Eqs. S9 and S10:

$$\Xi_{aq} = \exp(-\beta G_H)\,(1+10^{X})^{M}. \qquad [1]$$

Here, β is the inverse thermal energy and G_H is the hydrophobic free energy (>0) penalty to transfer a polymer from its hydrophobic reference state to the situation where the polymer is in contact with water. It is worth noting that this penalty will also encapsulate other free energy changes when the environment of the chain changes, such as differences in conformational entropy. The hydrophobic reference state can be the collapsed globule state of a single polymer chain or it can be the polymer as part of a large(r) aggregate with other chains. It can also be the interior of a micelle that can be formed if the hydrophobic polyelectrolyte is linked to a hydrophilic block, Fig. 1 for illustration. For carboxyl groups with hydroxyl "ligands," we have $X = pH - pK_a$, with $pK_a = -^{10}\log K_a$, K_a being the dissociation constant of a (solvated) carboxyl group. For basic groups, $X = pK_a' - pH$, with $pK_a' = -^{10}\log K_a'$, K_a' being the dissociation constant for the conjugate acid of the basic group. The value of M should be seen as the maximum number of ionizable groups affected by the transition under the relevant conditions in terms of pH and ionic strength. Coulomb interactions are expected to lead to values of M that are significantly smaller than the number of ionizable groups on the polymer, see, e.g., ref. 11. The statistical weight of the reference hydrophobic state is given by $\Xi_H \approx 1$. With the full grand partition function $\Xi = \Xi_{aq} + \Xi_H$, the fraction of polymer in the hydrophobic and aqueous state is given by

$$f_H = \Xi_H/\Xi = \left(1+\exp(-\beta G_H)(1+10^{X})^{M}\right)^{-1} \quad \text{and } f_{aq} = 1 - f_H. \qquad [2]$$

The fraction of ionized carboxyl or basic groups is given by, *SI Appendix*, Eq. S6 for derivation,

$$\theta = \frac{\langle N\rangle}{M} = \frac{10^{X}}{1+10^{X}} f_{aq}. \qquad [3]$$

The value of M in the equations above is a measure for the cooperativity ($M = 1$ implies no cooperativity) and determines the steepness of the transition, in this case, the pH range where the transition takes place, from the aqueous to the hydrophobic state or vice versa. This behavior is illustrated in Fig. 2 for an HPE with equal numbers of hydrophobic and ionizable groups.

The equations above assume uncorrelated ionizable groups, which is reflected in a single value for the ionization constant. However, as mentioned above, Coulomb interactions will inevitably lead to a spread of this constant. We may interpret the equations, therefore, as capturing only the differences between the state of the polymer around the transition and not as an

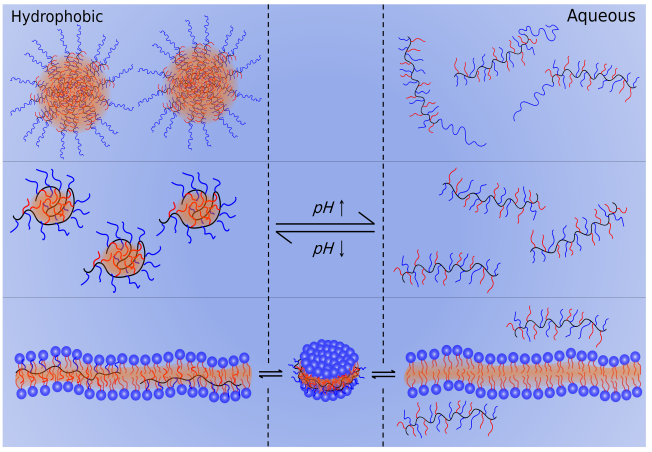

Fig. 1. Schematic illustration of a series of different possible states of an acidic hydrophobic polyelectrolyte in an aqueous solution. Changes in *pH* will lead to changes in the conformation or environment of the chains. *Top*, Micellization of a hydrophilic–hydrophobic polyelectrolyte diblock. *Middle*, Coil–globule transition. *Bottom*, Membrane permeation and solubilization. We may broadly partition them into "hydrophobic" and "aqueous" states, with a membrane nanodisk as an intermediate state. Red and blue polyelectrolyte side groups represent hydrophobic and hydrophilic (acidic) molecular moieties, respectively. Orange shading highlights the hydrophobic reservoirs that stabilize these hydrophobic side groups.

*A proton hole is also an equivalent ligand choice.

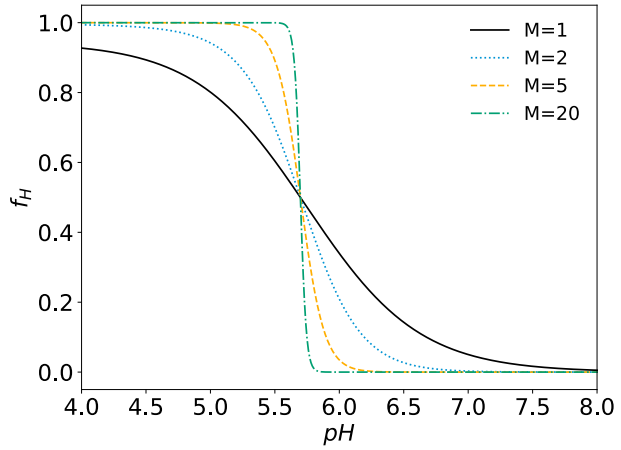

Fig. 2. Plots of HPE conformational transitions from a hydrophobic to aqueous state, f_H, Eq. **2**, for different degrees of cooperativity, M, in between 1 and 20. The number of ionizable acidic groups M is equal to M_H, the number of hydrophobic groups. Further, $pK_a = 4.5$, and $G_H = M_H g_H$, where $\beta g_H = 2.82$. Increasing g_H shifts the transition to higher pH for acidic groups.

absolute description of the ionization state of the chain. In other words, around the transitions, we approximate correlations by assuming that at most only a single chargeable group is ionized over a length of approximately the Bjerrum length (≈0.72 nm in water). We emphasize that this approximation holds in this case as further ionization beyond the point where the HPEs are overwhelmingly in the aqueous state does not influence the transition. Including correlations explicitly in the theory at this point is a significant challenge, in particular as intermediate states of the HPEs (besides hydrophobic, aqueous, and disk) are expected. The pH at which the transition takes place is, in this model, determined by the values of pK_a or pK_a' and G_H. The last quantity is expected to be an increasing function of the number of hydrophobic (side) groups of polymers that contain separate hydrophobic and ionizable groups, which has indeed been assumed in Fig. 2. In the case of polymers that contain more than one type of hydrophobic (side) group, G_H is expected to be a linear combination of the fraction of hydrophobic groups and their separate hydrophobic free energy contribution. As mentioned in the introductory section, when mixed with lipid bilayer membranes in the form of unilamellar or multilamellar vesicles, several hydrophobic polyelectrolytes spontaneously induce the formation of disks of roughly 10 nm in diameter throughout a well-defined pH range (2, 12, 13). The polymers are thought to adsorb at the rims or the disks; Fig. 1, *Bottom* row, where the hydrophobic parts of the polymers stick into the hydrophobic interbilayer spacing and the ionic groups preferably orient toward the outside, thereby maximizing contact with water. More complex hydrophobic polyelectrolytes (14–16) and peptides (17, 18) also destabilize membranes, probably by other mechanisms. So-called "membrane scaffold proteins" (MSP) (19–22) can also form disks but only after treatment with detergents. Mixtures of two lipids with different sizes or lipid with surfactant can also form disk-shaped aggregates on the order of tens of nanometers in size. These aggregates, where the smaller lipids or surfactant are located near the rims of the disks, are referred to as "bicelles" (23) and can form upon appropriately mixing the components. We define a third conformational state of the polymer when adsorbed onto disks. In the disk state, we assume that the hydrophobic parts of the polymer still pay a penalty for being at a hydrophobic–aqueous interface but that this penalty should be significantly smaller than for being fully in the aqueous state. As explained in *SI Appendix, Theory*, on average, less chargeable groups may get ionized compared to the situation where the polymers are fully dissolved in the aqueous state. Considering only carboxyl ionic groups, the resulting grand canonical weight of HPEs bound onto a bilayer disk is given by

$$\Xi_D = \exp(-\beta G_{HD})\,(1 + 10^{pH-pK_a})^{M_D}, \qquad [4]$$

where G_{HD} stands for the hydrophobic penalty of an HPE chain when adsorbed onto a disk which includes the formation free energy of the disk (per HPE chain) and M_D is the number of chargeable groups on the HPE in the disk state. The value of G_{HD} is expected to be a fraction of the value of G_H in Eq. **1**. $(M - M_D)/M$ should be seen as the fraction of time chargeable groups spend inside or close to the hydrophobic bilayer region. This is analogous to adding an additional term in Eq. **4** of the form $(1 + 10^{pH-pK_a^*})^{M-M_D}$, with $pK_a^* >> pK_a$. We will see later that for the particular hydrophobic polyelectrolytes we consider, the fraction of nonionized groups can be very small (<0.1). Alternatively, there may be an additional structural contribution to that fraction based on the architecture of the polymers. Moreover, the pK_a of the available ionized groups may be different from the one in the unconstrained aqueous form due to electrostatic repulsion with the lipid head groups. Note that if $M_D = M$, disks are always stable with respect to the aqueous state as $G_{HD} < G_H$ and therefore the statistical weight $\Xi_D > \Xi_{aq}$; Eqs. **1** and **4**. The ionized fraction now reads, *SI Appendix*, Eq. S6,

$$\theta = \frac{10^X}{\Xi}\left(\frac{M_D}{M}\exp(-\beta G_{HD})\left(1+10^X\right)^{M_D-1} + \exp(-\beta G_H)\left(1+10^X\right)^{M-1}\right). \quad \text{(presence of disks)}. \qquad [5]$$

In Eq. **5**, $\Xi = \Xi_{aq} + \Xi_H + \Xi_D$.

Comparison to Experiments

Diblock Micelles. An excellent example of a well-defined system which incorporates HPEs is the family of polymers investigated by Gao et al. (24–27). They synthesize diblock copolymers where one of the blocks is a cationic hydrophobic polyelectrolyte based on tertiary amines. Reference 25 includes fluorescent quenching data for a series of poly(ethylene oxide)-b-poly(2-(dipropylamino) ethyl methacrylate)-r-poly(2-(dibutylamino) ethyl methacrylate) (PEO-b-PDPA-r-PDBA) random copolymers (Inset in Fig. 3*B*), the fluorescence correlating with the dissolution of the micelles at low pH (Fig. 1, *Top* row for a schematic of the transition). The series of polymers have different DPA to DBA ratios (i : j) which affect their transition pH. From Fig. 3, reproduced from their work, we can observe sharp transitions for a series of different compositions. The pH range in which the transition occurs is over approximately 0.2 pH units, which is remarkably sharp and points to a highly cooperative transition (indeed $M \approx 11$, see later). To compare, a typical monomer analog of an HPE, butyric acid in a demixed system of octanol and water, undergoes a transition from mainly soluble in octanol to mainly soluble in water over a pH range as broad as roughly 4 pH units (28), which also is obvious in Fig. 2 for $M = 1$. It can also be seen in Fig. 3*A* that upon increasing the fraction of the most hydrophobic group in the polymers, the transition from an aqueous coil to a micelle (hydrophobic) state occurs at decreasing pH.

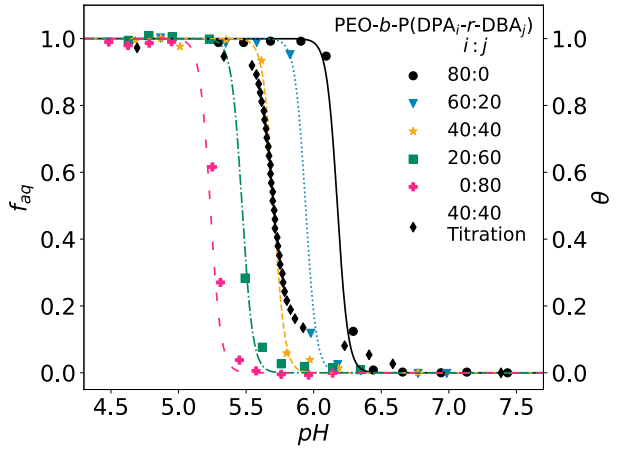

(A) Fitted f_{aq} (Eq. (**2**)) curves and θ (for 40:40 ratio, black rhombuses) curves (Eq. (**3**)). Note the strong correlation between the ionized and aqueous fraction in the middle curve (40:40 data). Global parameters: $M = 11$, $g_{DBA} = 11.2k_BT$ and $g_{DPA} = 9.0k_BT$. $pK'_a = 10.1$ from (26).

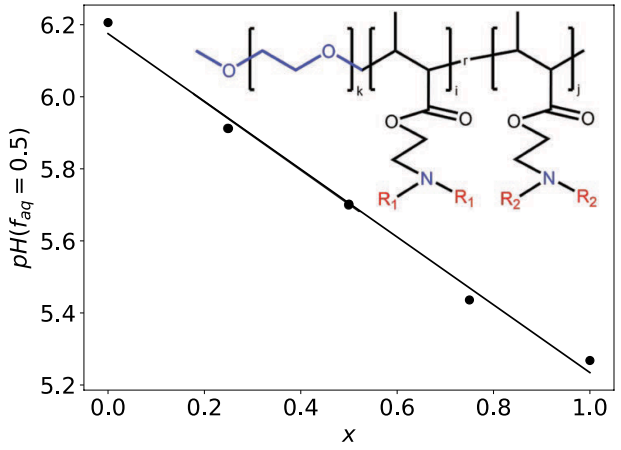

(B) Transition pH trend with respect to DBA mole fraction in the HPE block (x), fit with Eq. (**6**) using $pK'_a = 10.1$ from (26).

Fig. 3. Analysis of PEO-b-PDPA-r-PDBA micellization data from ref. 25. (*A*) Fluorescent and titration data. (*B*) Transition *pH* trend. Inset, Chemical structure of the polymer.

The aliphatic chains on this amine are varied to impart different degrees of hydrophobicity, therefore allowing for control over the transition pH. Due to the hydrophilic PEO block, there is a drive to form well-defined micelles, which we denote as the hydrophobic state in this system. In other words, the hydrophilic blocks prevent the formation of macroscopic aggregates and stabilize the HPE in their hydrophobic state in the cores of well-defined micelles. These will form at a pH high enough for the amines to become deprotonated in the core of the micelle. Conversely, the micelles fall apart as the pH is lowered, and the ionization of the HPE blocks is favored, leading to an increased solubility in the aqueous solution. We compare our model in the form of Eqs. **2** and **3** to the experiments in Fig. 3*A*. The structure of the hydrophobic polyelectrolyte indicates that the number of ionizable acidic groups M is equal to M_H, the number of hydrophobic groups ($M_H = M$). As explained in *SI Appendix, Theory*, we can describe the hydrophobic penalty, G_H, as a linear combination of the hydrophobic penalty for the two types of monomers via $G_H = Mf(g_{DBA}, g_{DPA}, x)$. Here, $f(g_{DBA}, g_{DPA}, x) = xg_{DBA} + (1 - x)g_{DPA}$. $g_{DBA}$and g_{DPA} are the hydrophobic free energy contributions per butyl and propyl monomer, respectively, and x is the mole fraction of DBA side groups in the hydrophobic polyelectrolyte. An important property of the diblock copolymer micelles is their transition pH, which we define as $\Xi_H = \Xi_{aq}(= 1)$, leading to $f_{aq} = 0.5$ and the following expression:

$$pH_{\text{micellization}} = pK'_a - 0.4343\beta f(g_{DBA}, g_{DPA}, x). \quad [6]$$

Here, we further used that at the transition, $10^{pKa'-pH} >> 1$. The numerical factor $0.4343 \approx 1/\ln 10$. A pK'_a of 10.1 was taken (26). There is an excellent agreement between this linear approximation and the experimental data; as shown in Fig. 3*B*, transition pH for different compositions can be easily calculated. Therefore, copolymerizing monomers with different hydrophobicities is an excellent method to target specific transition pH values, as also pointed out in ref. 25. Introducing the extracted values of G_H into Eq. **2** and using an average value of M calculated from a preliminary free parameter fit leads to the theoretical curves shown in Fig. 3*A*. Again, the general shape of the data is adequately described. Eq. **3** describes the relationship between f_H (and f_{aq}) and the ionization state of the polymer. In the language of MWC theory, protonation is similar to the binding of ligands, which in turn drives the conformation transition from a micelle (unbound to protons) to an aqueous (bound to at least several protons) state. Therefore, in MWC theory, ionization and aqueous fraction are predicted to be strongly correlated. This correlation has been illustrated for oxygen binding onto hemoglobin in *SI Appendix*, Fig. S1. In terms of our version of the theory, the factor relating f_{aq} and θ, $\frac{10^{pK'_a-pH}}{1+10^{pK'_a-pH}}$ (for a basic polyelectrolyte), will be close to unity at pH values a couple of units below the pK'_a, where most transitions take place. Therefore, we expect a similar transition both in sharpness and transition pH to be present for both titration and fluorescence data. Comparison of titration and fluorescence data from ref. 25 in Fig. 3*A* indeed shows good correspondence between both transitions. There is a strong correlation between the ionization state of the polymer and the conformational state of the chain, integral to the model we propose. The overlap of both of the transitions is however not perfect. There is a clear increase in ionization fraction of the polymer before the micelle dissolves. This behavior may arise due to outer groups on the HPE block becoming partially charged before the groups in the core. The value of M refers to the number of groups which change their ionization state during the transition. From Fig. 3, it is clear that the polymer goes from mainly ionized to mainly deionized during the transition. If ionization (protonation) was uncorrelated, which probably is the most severe approximation that we used, and in the absence of other broadening effects, the fitted value of M would be equal to the number of ionizable groups on the polymers, in this case, 80. The average fitted value of M is however around 11. Correlations due to Coulomb interactions will lead to a significant fraction of ionizable groups that remain uncharged around the pH where most micelles have dissolved. Other reasons for this effective widening of the transition are that roughly 20% of the polymer is already ionized before the micelles start dissolving. The two-state model relies on the assumption that there are solely two distinct environments for the chain. In reality, there will most likely be intermediate states between the two extremes of the micelle and the single chain. This will widen the transition. In the model proposed, this would correspond to states with slightly different G_H values. A system with one intermediate state is investigated

in *SI Appendix, Influence of Intermediate States on Transition Broadening*. There also might be experimental reasons for some broadening, but these are expected to be small, if only because hardly any hysteresis has been observed in these systems (26). In other words, the ionization of the micelle system is identical during the formation and dissolution of the micelles. Next, we test the prediction from Eqs. **2** and **3** that the coil–micelle transition becomes more cooperative (sharper) upon an increasing number of ionizable groups M or chain length. In refs. 26 and 29 Gao et al. present a system of diblock poly(ethylene oxide)-b-poly(2-(dibutylamino) ethyl methacrylate) (PEO-b-PDBA) polymers containing a hydrophilic block and a hydrophobic polyelectrolyte whose chain length (i) is varied (Inset in Fig. 4*B*). The data, in the form of titrations, are presented in Fig. 4*A*. This is a similar system to the one described above; however, as the composition of the side groups is constant here, one would expect from Eq. (**6**) that the transition pH is independent of chain length. That clearly is not the case; as can be seen in Fig. 4*B*, the transition pH, defined as the pH where $\theta = 0.5$, decreases over roughly 0.5 pH units when the number of monomers per chain increased from 5 to 100, the effect being largest for the shorter polymers. We postulate that this systematic change with length is caused by finite-size effects due to the hydrophobic groups that are close to the hydrophobic–aqueous interface. The groups on the HPE blocks neighboring the hydrophilic blocks experience a higher polarity environment than the groups that are further away from the junction and are immersed in the center of the core of the micelle. This can be accounted for by writing $G_H = g_H(M - b)$, where the value of b represents the portion of the polymer that sits close to the hydrophilic–hydrophobic junction or micelle interface. The value of b is expected to be smaller than unity, that is, a fraction of a monomer unit. So, we modify Eq. **6** into

$$pH_{\text{micellization}} = pK_a' - 0.4343\beta g_H \frac{M - b}{M}. \qquad [7]$$

This approach leads to a good description of the transition pH (Fig. 4*B*), and incorporating this expression for G_H into Eq. **3** allows us to fit the transitions adequately (Fig. 4*A*). In this case, a separate effective value of M is fit to each curve.

The values of M that follow from the fits of the experimental data in Fig. 4 to Eq. **3** again are significantly smaller than the number of ionizable groups, being consistent with the analysis of the data in Fig. 3. However, the trend illustrated in the inset of Fig. 4*A* is clear: Already with a chain length as short as 5 monomers, the transition is cooperative with $M \approx 1.8$ (no cooperativity corresponds to $M = 1$). At the longest chain of 100 monomers, we find $M \approx 45$. While it is unclear at this point what causes the large increase in effective M value in between chain lengths of 60 and 100 monomers, the increased level of cooperativity as a function of chain length is consistent with the trend predicted by theory. The significant cooperativity of the transitions on the basis of Fig. 4*A* was also concluded in ref. 26, based on the Hill coefficient (30). As Hill isotherms are empirical and can reflect many mechanisms (30), the added value of the analysis here is that the cooperative nature of the transition is shown to be coupled to the conformations of the polymers via an MWC-like mechanism. All of this combined constitutes the most complete proof of an MWC-like transition in relatively simple (macro)molecules that is currently available from existing data in the literature. That, in turn, leads to the question of whether all transformations induced by pH in HPEs are consistent with the MWC model. As will be illustrated below for the single-chain globule–coil transition in HPEs, that is not always the case, at least not convincingly.

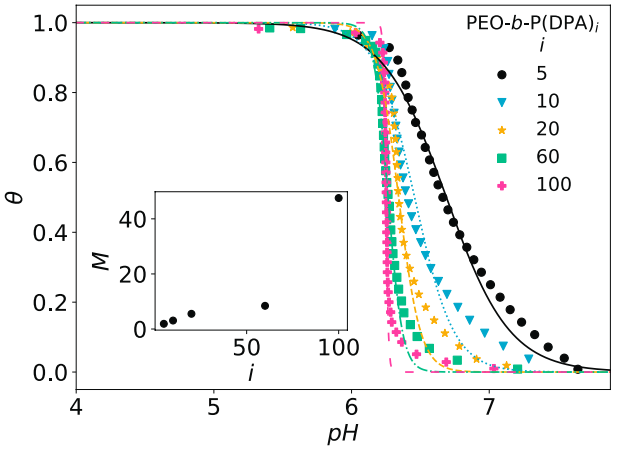

(A) Fit of the titration data using Eq. (**3**) for different lengths (i) of DPA blocks in PEO-b-PDPA diblocks. Local parameters: $M = 1.8, 3.1, 5.5, 8.4, 45.3$ for the 5, 10, 20, 60 and 100 lengths respectively. Values of G_H are calculated from Eq. (7) with global paremeters: $b = 0.60$, $g_H = 0.9k_BT$. $pK_a' = 10.1$ from (26). Inset: Fitted M against DPA block length (i) trend.

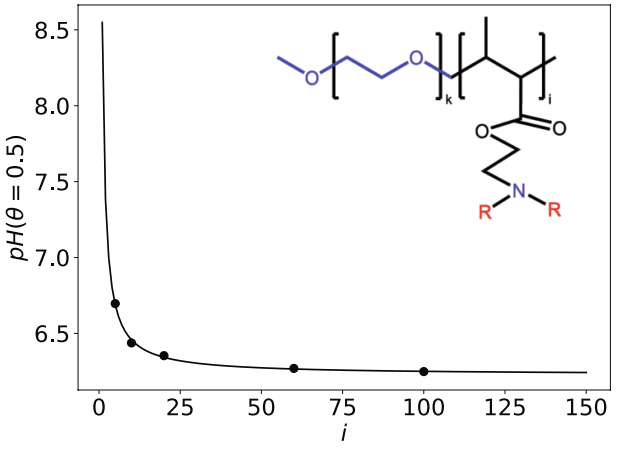

(B) Fit, using Eq. (**7**), of the transition pH with respect to DPA block length (i). $M = i$ was set in Eq. (**7**). Global parameters: $b = 0.60$, $g_H = 0.9k_BT$. $pK_a' = 10.1$ from (26).

Fig. 4. Analysis of the effect of PDPA block length on PEO-b-PDPA titration data from ref. 26. (*A*) Titration data. (*B*) Transition *pH* trend. Inset, Chemical structure of the polymer.

Coil–Globule Transition. The coil–globule transition is, a priori (and perhaps naively), the most basic example of a two-state system we may consider (Fig. 1, *Middle* row). However, at least in (slightly) hydrophobic polyelectrolytes, the debate still continues after the early work of Mandel et al. (31) and Koenig et al. (32) in the late 1960s. A more recent attempt to pin down the nature of the coil–globule transition in poly(methacrylic acid) (PMAA) was reported by Ruiz et al. (33). They effectively look at the transition at different length scales by comparing rotational correlations (monomer scale) and hydrodynamic radii (full polymer scale).

We combine the data from ref. 33 with those on poly(ethylacrylic acid) (PEAA) in ref. 34 in Fig. 5. There, we also add the measured ionization fractions θ obtained by titration from ref. 11 (Fig. 5*A*) and ref. 35 (Fig. 5*B*). To apply the analysis described in the previous section to the experimental data, those

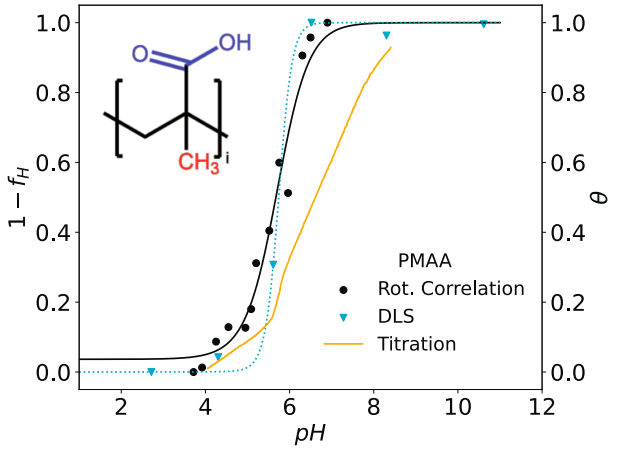

(A) PMAA: Fits, using Eq. (**2**), of rotation correlation data (black) (parameters: $M = 1.2$, $g_H = 2.8k_BT$) and dynamic light scattering (DLS) data (cyan) (parameters: $M = 2.9$, $g_H = 2.9k_BT$). $pK_a = 4.5$ is assumed. Titration (θ) data is shown in orange.

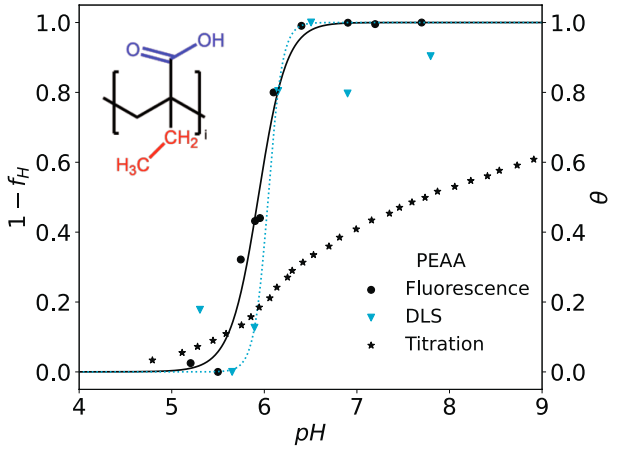

(B) PEAA: Fits, using Eq. (**2**), of pyrene probe fluorescence data (black) (parameters: $M = 3$, $g_H = 3.3k_BT$) and dynamic light scattering (DLS) data (cyan) (parameters: $M = 6$, $g_H = 3.6k_BT$). $pK_a = 4.5$ is assumed. Titration (θ) data is shown as black stars.

Fig. 5. Coil–globule transitions for (*A*) PMAA and (*B*) PEAA as a response to solution *pH* changes. These data were obtained from refs. 33 and 11 and refs. 34 and 35, respectively. Insets, Chemical structure of the polymers.

were scaled and translated into a hydrophobic fraction. The rotation correlation spectroscopy data, which probes local viscosity in a molecule, can be directly translated into a hydrophobic fraction by taking the maximum and minimum correlation times as $f_H = 1$ and $f_H = 0$. In the case of the hydrodynamic radii (DLS) data, this assignment is reversed. When applying Eq. **2**, with $G_H = g_H M_H$ and $M = M_H$, we find fitted values of M for the correlation and scattering data to be 1.2 and 2.9, respectively; Fig. 5*A*. This is in stark contrast to the number of repeating groups that compose the polymer, around 1,000 and with the results obtained from micellization in the previous section, which points to values of M of the same order of magnitude as the number of ionizable groups. It is worth noting, just as the authors have too, that there is not enough data in the transition region for the scattering data to be confidently fit however.

In Fig. 5*B*, the similarly scaled dynamic light scattering and pyrene probe fluorescent measurements from ref. 34 have been plotted. The maximum and minimal values of the fluorescent intensity are taken as $f_H = 1$ and $f_H = 0$, while this assignment is again reversed for the hydrodynamic radius data. Both sets of data present a very similar transition *pH* and similar steepness in the curves. The fitted values of M are 3 and 6 for the fluorescence and scattering data, respectively, which is again considerably lower in order of magnitude than the number of carboxylic acid groups per chain, which is around 360. As expected, the hydrophobic energy per group is lower for the PMAA than the PEAA, which is reflected in the lower transition *pH*. In both cases, there is a very significant difference (2 to 3 orders of magnitude) between the effective value of M and the number of repeating groups on the chains. As mentioned in the last section, the value of M does not mirror the number of repeating units but rather the ionization change during the transition. When comparing the θ and $1 - f_H$ curves, it is clear that the two quantities are not that well correlated. As the *pH* is reduced, a significant amount of the polymer becomes deprotonated before the transitions take place. This reduces the effect of the ionization change on the steepness of the transition. Moreover, a spreading out of the coil–globule transition with respect to *pH* might be expected due to the assumption that there is a clear-cut conformation change. As convincingly shown in ref. 36, a cascade of different conformations are seen (by computer simulation), such as so-called pearl-necklace conformations with local "pearls" of collapsed states that are connected via ionized strings of the polymers (1, 37, 38). Several of these states are present between the limiting coil and globule conformations (36). *SI Appendix, Influence of Intermediate States in Transition Broadening* for further discussion. For single chains (and the associated globules), there will be a significant proportion of surface groups with respect to groups in the bulk of the aggregate. This allows for some of the ionic groups to remain ionized even when in the globule state, reducing the value of M. Although there are indications, as has been noted extensively in the literature, that the coil–globule transitions of hydrophobic polyelectrolytes are to a certain extent cooperative, they do not seem to warrant a two-state treatment. A progressive transition including several intermediate states seems more likely. From these results, we conclude that the coil–globule (-like) transition in the HPE has the rudimentary signature of a cooperative transition, but it is not in agreement with the MWC mechanism based on two conformation states where strong(er) coupling between conformation states (f_H) and ligand binding (ionization state θ) is predicted. In contrast, in the situation with micelles formed by diblocks, the HPE blocks in the micelle cores correspond to a well-defined conformation that is clearly distinguishable from the aqueous coil state in the diblock system. We conclude from this comparison that intrinsic or other conditions are necessary to select well-defined conformation states. Such intrinsic condition can be "programmed" in the architecture of the HPE, in this case, in the form of HPEs being linked to hydrophilic blocks so that aggregation in the form of micelles is preferred over several intermediate states such as those in the coil–globule transition as illustrated in ref. 36. A micelle interior can be seen as a reservoir that stabilizes the hydrophobic conformational state of the HPE. In principle, hydrophobic reservoirs can also be provided by other species that may stabilize one or more conformation states of the HPE (Fig. 1). In the next section, we will show that the presence of lipid bilayers, in the form of (single or multilamellar) vesicles, can provide conditions in the form of reservoirs to select well-defined conformation states of the HPE.

Membrane Solubilization by Disk Formation. Many hydrophobic polyelectrolytes are known to interact with lipid bilayer membranes (16). Depending on the hydrophobicity, chemical

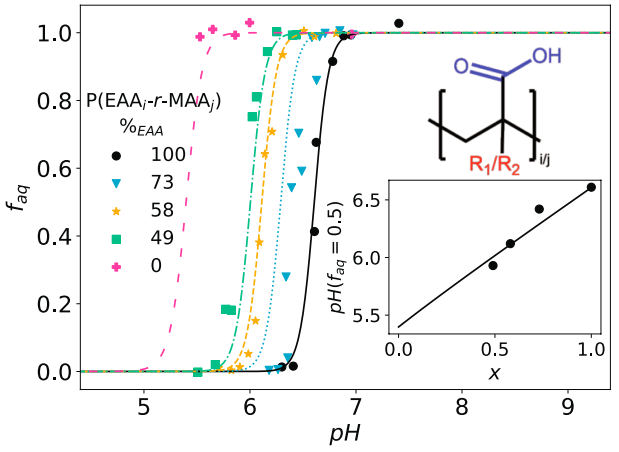

(A) Fitted f_{aq} curves (Eq. (**9**)). Global parameters: $M = 65$, $\Delta g_{EEA} = 0.49 k_B T$, $\Delta g_{MAA} = 0.22 k_B T$ and $\frac{M_D}{M} = 0.9$. pK_a = 4.5 is assumed. Inset: transition pH trend with respect to the EAA mole fraction of the polymer (x). Fitted using Eq. (8).

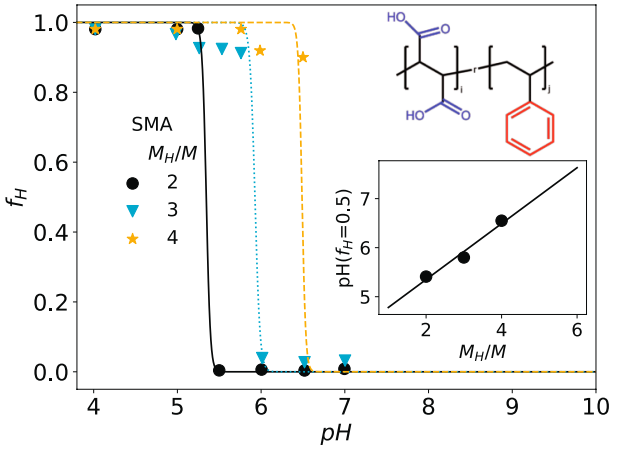

(B) Fitted f_H curves (Eq. (**11**)). Local parameters: $M = 19.5, 14.8, 20$ for the $\frac{M_H}{M} = 2$, 3 and 4 variants respectively. Global parameters: $g_H = 1.28 k_B T$ and $pK_a = 4.3$. Note $M_H/M = j/i$. Inset: transition pH fitted with Eq. (**10**).

Fig. 6. Membrane dissolution data for (*A*) PEAA-PMAA (35) and (*B*) SMA (13). The chemical structures of the polymers are given as insets.

structure, and relative concentration of the HPE, membranes exhibit solubilization or fusion among other destabilization mechanisms. These processes, usually triggered via a pH change, tend to be coupled to the release of the contents of the membrane, leading to the interest in such systems for drug delivery applications. Styrene–maleic acid (SMA) is used to make nanometer-sized (~10 nm) vesicle nanodisks which allow for the study of membrane proteins in their local environments (39–41). Fig. 1, *Bottom* row shows a schematic of a disk and the states of an HPE in such a system. Tirrell and coworkers showed in a series of papers the solubilization of different types of lipid vesicles by poly(ethylacrylic acid)-r-poly(methylacrylic acid) copolymers (PEAA-r-PMAA) (35). In Fig. 6, we summarize the findings in refs. 35 and 13 for these different HPEs.

The stabilization of a nanodisk phase can be seen as analogous to the stabilization of any hydrophobic–hydrophilic interface, albeit one with a high curvature. Therefore, we can expect the hydrophobic polyelectrolyte to act like a surfactant with the hydrophobic groups directed toward the core of the nanodisk and the carboxyl groups pointing out into solution. This mechanism relies on the two moieties being able to freely rotate with respect to the chain backbone, as in styrene–maleic acid copolymers, or being located on different branches of the same monomer. The family of poly(alkyl acrylic acid) polymers falls under that category. *SI Appendix*, Table S1 for a comparison of some HPE structures. Tirrell et al. describe the pH-dependent solubilization of DPPC multilamellar membranes using PEAA-r-PMAA copolymers with a chain length of around 2,000 for all of the polymer compositions. They focus on the tunability of the transition pH on changing the EAA to MAA ratio in the polymer. Turbidimetry was used to monitor the dissolution of the membranes as a function of pH. The measurements are normalized to the value measured before the solubilization transition where unperturbed membranes are present. Therefore, assuming no intermediate structural changes other than disk formation, the turbidity measured directly correlates with the fraction of membranes that remain undissolved. Only the aqueous–disk transition was investigated; therefore, only the difference in hydrophobic penalty between the solubilized polymer and the polymer at the disk solvent interface is needed to characterize the system. In the absence of the usual reference for the hydrophobic penalty, that is, the penalty in the hydrophobic state, only a difference in hydrophobic penalty between the aqueous and disk state can be extracted. This is analogous to making the disk state the reference state.

The pH at which the transition from the disk to the aqueous state takes place, pH_{DA}, follows from setting $\Xi_{aq} = \Xi_D$ in Eqs. **1** and **4**, which leads to $pH_{DA} = pK_a + \frac{0.4343\beta(G_H - G_{HD})}{(M - M_D)}$. We write the hydrophobic free energy difference between the aqueous state and the disk conformation as a function of composition via $G_H - G_{HD} = M_H f(\Delta g_{EAA}, \Delta g_{MAA}, x)$. Here $f(\Delta g_{EAA}, \Delta g_{MAA}, x) = x\Delta g_{EAA} + (1 - x)\Delta g_{MAA}$, where Δg_{EAA}, Δg_{MAA} are the hydrophobic free energy differences between the aqueous state and disk conformation per monomer, and x is the mole fraction of EAA in the polymer. Combining all that leads to (note that we have $M_H = M$ here)

$$pH_{DA} = pK_a + \frac{0.4343\beta f(\Delta g_{EAA}, \Delta g_{MAA}, x)}{1 - \frac{M_D}{M}}. \qquad [8]$$

The midpoints of the transition are found using a trial fit of the data, where $G_H - G_{HD}$ and $M - M_D$ are free parameters, Eq. **9** below. A value of 4.5 is assumed for the pK_a. We fixed $M_D/M = 0.9$, which is purely an assumption: 10% uncharged groups in the disk conformation compared to the aqueous state seems a reasonable upper limit. With that, a value for Δg_{EEA} is trivially found using the midpoint value for x=1, and linear regression can be used to find the value of Δg_{MAA} from Fig. 6*A*. Inserting the derived hydrophobic penalty values and the assumed value of the pK_a, we calculate the disk (and aqueous) fraction by

$$f_D = 1 - f_{aq} = \Xi_D/(\Xi_{aq} + \Xi_D)$$
$$= \left(1 + \exp[\beta(G_{HD} - G_H)](1 + 10^{(pH - pK_a)})^{(M - M_D)}\right)^{-1}. \qquad [9]$$

In calculating the fractions, we used an average effective value of $M - M_D$ = 6.5. The value of M cannot be extracted independently at this point. The match between the fitted transition and the experimental data is reasonable although not as good as in the micelles in Fig. 3. This is because there are stronger deviations from the linear relation between transition pH and x, as can be seen in the inset in Fig. 6*A*. Scheidelaar et al. report the solubilization of DMPC by styrene–maleic acid

random copolymers of different compositions (13). The disk-to-interbilayer spacing (hydrophobic) transition is remarkably sharp, considering that the average length of the polymers is of a few tens of units. The data clearly demonstrate how oligomeric species are also capable of extremely sharp pH-induced transitions. We find the transition pH for polymers with a ratio of styrene over maleic acid M_H/M by using Eq. **4** and setting $\Xi_D = \Xi_H = 1$. Taking $G_{HD} = M_H g_{HD}$ leads to

$$pH_{HD} = pK_a + 0.4343\beta g_{HD}\frac{M_H}{M}. \qquad [10]$$

The fraction of HPEs in the hydrophobic conformation, ignoring the weight of the aqueous conformation around this transition, is given by

$$f_H = \frac{\Xi_H}{\Xi_H + \Xi_D} = \left(1 + \exp(-\beta G_{HD})(1 + 10^{(pH - pK_a)})^{M_D}\right)^{-1}$$
$$\text{and } f_D = 1 - f_H. \qquad [11]$$

This analysis (Fig. 6*B*) follows the expected trend and yields a value for g_{HD} of $1.28 k_B T$ and an effective value of the pK_a of 4.3. The value for the effective pK_a is in good agreement with the pK_a of the first ionization of succinic acid, 4.21 (42) (note that maleic acid in the polymerized form in p(SMA) is structurally closer to succinic acid than to maleic acid). The second ionization of succinic acid has a higher pK_a of 5.6 and therefore might also play a role in these transitions, especially for the more hydrophobic polymers with higher values for the transition pH. In *SI Appendix*, we report a similar analysis of the (macroscopic) aggregation transition in SMA, also from ref. 13. There, an effective pK_a of 2.4 is found. However, as can be seen in *SI Appendix*, Fig. S3, the ionization and the aggregation state of the polymer are largely uncorrelated. A calculation of the effective pK_a for this system will not yield meaningful values with respect to the ionization state of the polymer. The analysis in *SI Appendix, HPE Aggregation* also reveals a value for the hydrophobic penalty relative to the aggregated state: $\beta g_H \approx 2.1$, which is significantly higher than the value of $\beta g_{HD} \approx 1.3$ that we find. A lower hydrophobic penalty g_{HD} is indeed expected due to the postulated penetration of the hydrophobic groups into the rims of the nanodisks. Note that this value also includes the work of formation of disks out of bilayer membranes. The effective values of M_D for the 2:1 and 3:1 variants were 19.5 and 14.8, respectively. Due to the overlap with what seems to be the aqueous–disk transition data, no attempt at estimating the sharpness was carried out for the 4:1 variant. The effective values of M_D point to a transition that is more cooperative (sharper) than the aqueous–disk transition in the PEAA-r-PMAA copolymers, despite the much longer chain length of the latter. While we cannot rule out other broadening effects, this effect is at least partly due to the fact that the sharpness of the aqueous–disk transition is governed by the difference $M - M_D$, Eq. **9**, while sharpness of the hydrophobic disk transition (as in SMA) is measured by the value of M_D, Eq. **11**. Finally, in comparison with the aggregation transition of SMA analyzed in *SI Appendix*, where we find values of M of 5.6, 4.9, and 12.0 for the 4:1, 3:1, and 2:1 styrene–maleic acid ratios, respectively, the hydrophobic–disk transition is significantly sharper. That again points to the requirement of well-defined reservoirs (in the form of bilayers) that are able to stabilize a finite number of conformational states (here the disk and presumably the hydrophobic state where the HPEs are dissolved in the interbilayer spacings). A comparison between the aqueous fractions and ionization states in the aggregation transition indeed reveals a similar lack of correlation as the situation for the globule–coil transition. In Fig. 7, the results in Fig. 6 are summarized and complemented with predicted scenarios for the hydrophobic-disk transition in Fig. 7, *Left*, and for the disk-aqueous transition in Fig. 7, *Right*. These predicted phase diagrams are based on (at this point) unverifiable choices for the hydrophobic contributions. We also show the predicted behavior of the ionized fraction Eq. **5**, again based on the assumption that 10% of the ionizable groups remain uncharged in the disk conformations.

The experiments in ref. 13 indicate that the aqueous–disk transition presents a much more noisy and much less sharp and well-defined transition compared to the hydrophobic–disk transition. This might be expected due to the ionization difference between the aqueous state and the disk state potentially

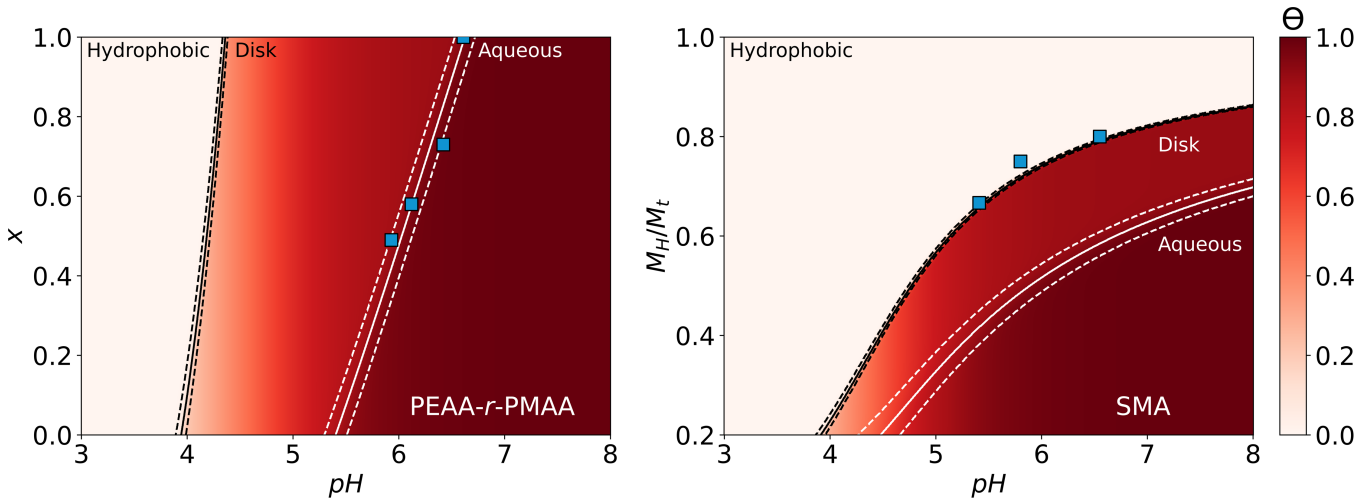

Fig. 7. Calculated phase diagrams for HPEs as a function of pH and composition for the PEAA-r-PMAA system (*Left*) and the SMA system (*Right*) using Eqs. **9** and **11**. Solid lines (black for the hydrophobic–disk transition and white for the disk–aqueous transition) denote the transition between the different phases and dotted lines where the main phase reaches a fraction of 0.9. Note the marked difference in transition steepness for the disk–aqueous versus the hydrophobic–disk transition. The blue squares are experimental data at the transition midpoints in Fig. 6. The red hue in the background of the figures reflects the ionization fraction, θ, Eq. **5**, of the HPE. Global parameters: *Left*, $g_{MAA} = 0.44 k_B T$, $g_{EAA} = 0.98 k_B T$, $G_{HD} = G_H/2$, $pK_a = 4.5$ and $M = 100$. x is the mole fraction of EAA in the polymer. *Right*, $g_H = 1.6 k_B T$, $g_{HD} = g_H/1.3$, $pK_a = 4.3$ and $M_H + M = M_t = 100$.

being small (10%) and is indeed confirmed in the theoretical "phase diagram" in Fig. 7, *Right*. The experiments in figure 6B in ref. 13 indeed seem to point to a broad transition at *pH* values above approximately 7. The prediction is that a longer chain length of SMA will lead to a sharper aqueous–disk transition. In order to pin down the values of the hydrophobic free energies and the uncharged fraction of ionic groups, the ionization state of the HPE around the transitions needs to be known. The experimental determination of that quantity is expected to be challenging as the ionization state of the head groups of the lipids that make up the bilayers is also expected to (slightly) depend on *pH*. In closing this section, we would like to mention that the MWC-like mechanism in this work has not been included in the term "cooperative" as discussed in ref. 43. There, the term "cooperative" has been reserved for situations where binding sites interact. We are aware that the terminology we use can be debatable. As we see it, the transitions we describe in this work occur, and only occur, because of the binding of several ligands at once, and the term "cooperative" therefore seems appropriate. We note that the influence of Coulomb interactions in weakening the transitions is a form of "negative cooperativity" due to interactions between bound ligands. Both types of cooperativity add up and contribute to the effective value of the degree of cooperativity *M* in the several scenarios that we investigated.

Conclusion

The examples laid out in the previous sections illustrate that the transitions carried out by hydrophobic polyelectrolytes can range from strongly to weakly cooperative. Analysis of the micellization transition in diblocks provides strong evidence that the underlying mechanism of the observed cooperativity is in agreement with the MWC model (6) that was originally designed to understand allosteric transitions. We verify here that the MWC model is more general: allostery, or interactions between binding sites, is not a requirement for the MWC model to work. What is required is the availability of two or more well-defined conformations with different affinity for ligands (here protons or hydroxyl ions). In the relatively simple substrates (at least compared to hemoglobin) studied here, the conformational states are coupled to hydrophobic or aqueous reservoirs. These reservoirs may be self-induced, such as in the case of micelles, or due to external structures being present, such as during the solubilization of bilayers. In the HPE, the conformational penalty in the aqueous and disk state is (within reasonable accuracy) a linear combination of the composition of the polymers. This can be clearly seen in Fig. 3 for the micellar systems and Fig. 6 for the disk formation. While this points to MWC as a plausible mechanism for disk formation, more quantitative comparison between theory and experiments is desired. Additional experiments to make that possible are for example the determination of the ionization states of HPEs in the disk and aqueous states, as shown in the form of predictions in Fig. 7, as well as the typical adsorption density of HPEs onto the disk rims. Moreover, for medical applications, it would be relevant to study the influence of temperature. In principle, the observed cooperativity as well as the ability to tune the transition *pH* in disk formation may provide a strategy to specifically target tumor cells; *SI Appendix*, *Applications* for a discussion of this possibility. There likely are several hurdles to overcome, for example, dilution effects and the unknown role of membrane proteins. The principles laid out in this work are not only applicable in "simple" HPEs but may also be applied in designing oligopeptides with combined hydrophobic and acidic (or zwitterionic) amino acids, see, e.g., refs. 44–46. These types of oligopeptides, often referred to as "cell-penetrating peptides" (18), depending on their architecture, may permeate cell membranes as a function of *pH* or by the concentration of ligands other than protons. Weakly cross-linked HPEs have also been observed to have a sharp *pH*-mediated transition: from a swollen (with water) to a collapsed state; see, e.g., refs. 47 and 48. We expect that there, the swollen state is analogous to the "aqueous" conformation, and the collapsed state is similar to the "hydrophobic" state in the previous sections. By being cross-linked, the occurrence of many intermediate conformations between the aqueous and hydrophobic states may be avoided. Potential applications of these systems are, for example, actuator, optical switches, and drug delivery vehicles that are driven by small *pH* variations. It should be noted that details can be important here as not all cross-linked HPEs have a narrow transition, see, e.g., ref. 49. There, cross-linked HPEs are being studied that consist of relatively strongly hydrophobic alkyl-acrylates with alkyl chain lengths between 8 and 18 carbon units, which may lead to local phase separation within the gels. In general, it is expected that (macro)molecular substrates that have multiple binding sites for ligands can undergo sharp transitions driven by small variations in ligand concentration. The degree of sharpness, or cooperativity, is largely determined by the stabilization of well-defined conformational states. Besides the acid–base systems analyzed in this work, we expect that other relatively simple host–guest systems (50) can have similarly sharp transitions. In these systems, the "hosts" are functional groups on (hydrophobic) oligomers or polymers and the "guests" are ligands.

Data, Materials, and Software Availability. Previously published data were used for this work (11, 13, 25, 26, 33–35).

ACKNOWLEDGMENTS. We thank Jinming Gao and Yang Li for kindly providing the data on HPE diblocks and Neshat Moslehi, Bas van Ravensteijn, and Tina Vermonden for discussions on hydrophobic polyelectrolytes. Antoinette Killian, Adrian Kopf, and Martijn Koorengevel are thanked for several illuminating brainstorming sessions on membrane disk formation. WKK thanks Rob Phillips and Tal Einav for enlightenment regarding MWC theory. Finally, we acknowledge the Dutch Research Council (NWO) for funding (grant no 712.018.003).

1. A. V. Dobrynin, M. Rubinstein, Hydrophobic polyelectrolytes. *Macromolecules* **32**, 915–922 (1999).
2. J. L. Thomas, S. W. Barton, D. A. Tirrell, Membrane solubilization by a hydrophobic polyelectrolyte: Surface activity and membrane binding. *Biophys. J.* **67**, 1101–1106 (1994).
3. R. Phillips, *The Molecular Switch - Signaling and Allostery* (Princeton University Press, 2020).
4. J. Berg, J. Tymoczko, L. Stryer, *Biochemistry* (Freeman and Co., ed. 7, 2011).
5. R. Phillips, J. Kondev, J. A. Theriot, H. G. Garcia, *Physical Biology of the Cell* (Garland Science, NY, ed. 2, 2013).
6. J. Monod, J. Wyman, J. P. Changeux, On the nature of allosteric transitions: A plausible model. *J. Mol. Biol.* **12**, 88–118 (1965).
7. R. C. Petter, J. S. Salek, C. T. Sikorski, G. Kumaravel, F. Lin, Cooperative binding by aggregated mono-6-(alkyl amino)-p-cyclodextrins. *J. Am. Chem. Soc.* **112**, 3860–3868 (1990).
8. F. J. Martinez-Veracoechea, D. Frenkel, Designing super selectivity in multivalent nano-particle binding. *Proc. Natl. Acad. Sci. U.S.A.* **108**, 10963–10968 (2011).
9. G. V. Dubacheva, T. Curk, D. Frenkel, R. P. Richter, Multivalent recognition at fluid surfaces: The interplay of receptor clustering and superselectivity. *J. Am. Chem. Soc.* **141**, 2577–2588 (2019).
10. M. Kanamala, W. R. Wilson, M. Yang, B. D. Palmer, Z. Wu, Mechanisms and biomaterials in pH-responsive tumour targeted drug delivery: A review. *Biomaterials* **85**, 152–167 (2016).
11. M. Mandel, J. C. Leyte, Potentiometric behavior of polymethacrilic acid. *J. Polym. Sci.: Part A* **2**, 1879–1891 (1964).
12. J. L. Thomas, D. A. Tirrell, Polyelectrolyte-sensitized phospholipid vesicles. *Acc. Chem. Res.* **25**, 336–342 (1992).
13. S. Scheidelaar *et al.*, Effect of polymer composition and pH on membrane solubilization by styrene-maleic acid copolymers. *Biophys. J.* **111**, 1974–1986 (2016).
14. F. Vial, A. G. Oukhaled, L. Auvray, C. Tribet, Long-living channels of well defined radius opened in lipid bilayers by polydisperse, hydrophobically-modified polyacrylic acids. *Soft Matter* **3**, 75–78 (2007).

15. F. Vial, F. Cousin, L. Bouteiller, C. Tribet, Rate of permeabilization of giant vesicles by amphiphilic polyacrylates compared to the adsorption of these polymers onto large vesicles and tethered lipid bilayers. *Langmuir* **25**, 7506–7513 (2009).
16. M. A. Yessine, J. C. Leroux, Membrane-destabilizing polyanions: Interaction with lipid bilayers and endosomal escape of biomacromolecules. *Adv. Drug Delivery Rev.* **56**, 999–1021 (2004).
17. Y. Takechi *et al.*, Comparative study on the interaction of cell-penetrating polycationic polymers with lipid membranes. *Chem. Phys. Lipids* **165**, 51–58 (2012).
18. D. M. Copolovici, K. Langel, E. Eriste, Ü. Langel, Cell-penetrating peptides: Design, synthesis, and applications. *ACS Nano* **8**, 1972–1994 (2014).
19. I. G. Denisov, S. G. Sligar, Nanodiscs for structural and functional studies of membrane proteins. *Nat. Struct. Mol. Biol.* **23**, 481–486 (2016).
20. I. G. Denisov, Y. V. Grinkova, A. A. Lazarides, S. G. Sligar, Directed self-assembly of monodisperse phospholipid bilayer nanodiscs with controlled size. *J. Am. Chem. Soc.* **126**, 3477–3487 (2004).
21. T. H. Bayburt, Y. V. Grinkova, S. G. Sligar, Self-assembly of discoidal phospholipid bilayer nanoparticles with membrane scaffold proteins. *Nano Lett.* **2**, 853–856 (2002).
22. C. R. Morgan *et al.*, Conformational transitions in the membrane scaffold protein of phospholipid bilayer nanodiscs. *Mol. Cell. Proteomics* **10** (2011).
23. U. H. Dürr, R. Soong, A. Ramamoorthy, When detergent meets bilayer: Birth and coming of age of lipid bicelles. *Prog. Nucl. Magn. Reson. Spectrosc.* **69**, 1–22 (2013).
24. K. Zhou *et al.*, Tunable, ultrasensitive pH-responsive nanoparticles targeting specific endocytic organelles in living cells. *Angew. Chem. - Int. Ed.* **50**, 6109–6114 (2011).
25. X. Ma *et al.*, Ultra-pH-sensitive nanoprobe library with broad pH tunability and fluorescence emissions. *J. Am. Chem. Soc.* **136**, 11085–11092 (2014).
26. Y. Li *et al.*, Molecular basis of cooperativity in pH-triggered supramolecular self-assembly. *Nat. Commun.* **7** (2016).
27. Y. Li *et al.*, Non-covalent interactions in controlling pH-responsive behaviors of self-assembled nanosystems. *Polym. Chem.* **7**, 5949–5956 (2016).
28. S. Rayne, K. Forest, pH dependent partitioning behaviour of food and beverage aroma compounds between air-aqueous and organic-aqueous matrices. *Flavour Fragrance J.* **31**, 228–234 (2016).
29. Y. Li, Y. Wang, G. Huang, J. Gao, Cooperativity principles in self-assembled nanomedicine. *Chem. Rev.* **118**, 5359–5391 (2018).
30. A. Hill, The possible effects of the aggregation of the molecules of haemoglobin on its dissociation curves. *Proc. Physiol. Soc.* **40**, iv–vii (1910).
31. M. Mandel, The conformational transition of poly(methacrylic acid) in solution. *J. Phys. Chem.* **71**, 603–612 (1967).
32. J. L. Koenig, A. C. Angood, J. Semen, J. B. Lando, Laser-excited Raman studies of the conformational transition of syndiotactic polymethacrylic acid in water. *J. Am. Chem. Soc.* **91**, 7250–7254 (1969).
33. L. Ruiz-Pérez *et al.*, Conformation of poly(methacrylic acid) chains in dilute aqueous solution. *Macromolecules* **41**, 2203–2211 (2008).
34. K. M. Eum, K. H. Langley, D. A. Tirrell, Quasi-elastic and electrophoretic light scattering studies of the reorganization of dioleoylphosphatidylcholine vesicle membranes by poly(2-ethylacrylic acid). *Macromolecules* **22**, 2755–2760 (1989).
35. J. L. Thomas, H. You, D. A. Tirrell, Tuning the response of a pH-sensitive membrane switch. *J. Am. Chem. Soc.* **117**, 2949–2950 (1995).
36. S. Ulrich, A. Laguecir, S. Stoll, Titration of hydrophobic polyelectrolytes using Monte Carlo simulations. *J. Chem. Phys.* **122**, 094911 (2005).
37. A. Kiriy *et al.*, Cascade of coil-globule conformational transitions of single flexible polyelectrolyte molecules in poor solvent. *J. Am. Chem. Soc.* **124**, 13454–13462 (2002).
38. P. M. Blanco, S. Madurga, C. F. Narambuena, F. Mas, J. L. Garcés, Role of charge regulation and fluctuations in the conformational and mechanical properties of weak flexible polyelectrolytes. *Polymers* **11**, 1962 (2019).
39. S. Tonge, B. Tighe, Responsive hydrophobically associating polymers: A review of structure and properties. *Adv. Drug Deliv. Rev.* **53**, 109–122 (2001).
40. T. J. Knowles *et al.*, Membrane proteins solubilized intact in lipid containing nanoparticles bounded by styrene maleic acid copolymer. *J. Am. Chem. Soc.* **131**, 7484–7485 (2009).
41. J. M. Drr *et al.*, The styrene-maleic acid copolymer: A versatile tool in membrane research. *Eur. Biophys. J.* **45**, 3–21 (2016).
42. D. Lide, *CRC Handbook of Chemistry and Physics* (CRC Press, ed. 86th, 2005–2006, 2005).
43. G. Ercolani, Assessment of cooperativity in self-assembly. *J. Am. Chem. Soc.* **125**, 16097–103 (2003).
44. T. M. Birshtein *et al.*, The models of the denaturation of globular proteins. III. *J. Plo. Sci.: Part C* **16**, 3533–3545 (1968).
45. E. V. Anufrieva, V. E. Bychkova, M. G. Krakovyak, V. D. Pautov, O. B. Ptitsyn, A synthetic polypeptide with a compact structure and its self-organization. *FEBS Lett.* **55**, 46–49 (1975).
46. Š Štokrová, M. Bohdanecký, K. Bláha, J. Šponar, Conformational transitions of leucine-containing isomeric sequential basic polytripeptides. *Biopolymers* **28**, 1731–1744 (1989).
47. R. A. Siegel, B. A. Firestone, pH-dependent equilibrium swelling properties of hydrophobic polyelectrolyte copolymer gels. *Macromolecules* **21**, 3254–3259 (1988).
48. R. A. Siegel, Hydrophobic weak polyelectrolyte gels: Studies of swelling equilibria and kinetics. *Adv. Polym. Sci.* **109**, 233–267 (1993).
49. O. E. Philippova, D. Hourdet, R. Audebert, A. R. Khokhlov, pH-responsive gels of hydrophobically modified poly(acrylic acid). *Macromolecules* **30**, 8278 (1997).
50. J. M. Lehn, *Supramolecular Chemistry: Concepts and Perspectives* (VCH Publishers, 1995).